environmental microbiology

Environmental Microbiology (2018) **20**(3), 1030–1040 doi:10.1111/1462-2920.14041

# Transformation of *Diplonema papillatum*, the type species of the highly diverse and abundant marine microeukaryotes Diplonemida (Euglenozoa)

**Binnypreet Kaur,[1,2] Matus Valach,[3] Priscila Peña-Diaz,[1] Sandrine Moreira,[3] Patrick J. Keeling,[4] Gertraud Burger,[3] Julius Lukeš[1,2] and Drahomíra Faktorová[1,2]***

[1]*Institute of Parasitology, Biology Centre, Czech Academy of Sciences, České Budějovice (Budweis), Czech Republic.*

[2]*Faculty of Sciences, University of South Bohemia, České Budějovice (Budweis), Czech Republic.*

[3]*Department of Biochemistry and Robert-Cedergren Centre for Bioinformatics and Genomics, Université de Montréal, Montreal, Canada.*

[4]*Botany Department, University of British Columbia, Vancouver, Canada.*

## Summary

***Diplonema papillatum*** **is the type species of diplonemids, which are among the most abundant and diverse heterotrophic microeukaryotes in the world's oceans. Diplonemids are also known for a unique form of post-transcriptional processing in mitochondria. However, the lack of reverse genetics methodologies in these protists has hampered elucidation of their cellular and molecular biology. Here we report a protocol for** ***D. papillatum*** **transformation. We have identified several antibiotics to which** ***D. papillatum*** **is sensitive and thus are suitable selectable markers, and focus in particular on puromycin. Constructs were designed encoding antibiotic resistance markers, fluorescent tags, and additional genomic sequences from** ***D. papillatum*** **to facilitate vector integration into chromosomes. We established conditions for effective electroporation, and demonstrate that electroporated constructs can be stably integrated in the** ***D. papillatum*** **nuclear genome. In** ***D. papillatum*** **transformants, the heterologous puromycin resistance gene is transcribed into mRNA and translated into protein, as determined by Southern hybridization, reverse transcription, and Western blot analyses. This is the first documented case of transformation in a euglenozoan protist outside the well-studied kinetoplastids, making** ***D. papillatum*** **a genetically tractable organism and potentially a model system for marine microeukaryotes.**

Received 3 November, 2017; revised 13 December, 2017; accepted 15 December, 2017. *For correspondence. E-mail dranov@paru.cas.cz; Tel. +420 387775433; Fax +420 385310388.

## Introduction

Diplonemids are biflagellate protists inhabiting marine ecosystems. Diplonemids, together with symbiontids (a small poorly studied group of species living in anoxic or low-oxygen marine environment, for which no molecular data are available [Breglia *et al*., 2010]), euglenids (important component of the freshwater ecosystems), and kinetoplastids (including free-living *Bodo*, as well as the highly pathogenic *Trypanosoma* and *Leishmania* spp.), form Euglenozoa. Both the kinetoplastids and euglenids have long been recognized as ecologically omnipresent and species-rich, while diplonemids were considered an insignificant group both in terms of diversity and ecology, and they remained poorly-studied (Lukeš *et al*., 2015).

The first diplonemid, *Diplonema breviciliata*, was described by Griessman in 1914 (Griessman, 1914), and only less than half a dozen species in two genera have been described since then (Skuja, 1948; Schuster *et al*., 1968; Porter, 1973; Larsen and Patterson, 1990; Schnepf, 1994; Simpson, 1997; Roy *et al*., 2007). More recent ecological surveys tracked down two clades of previously unrecognized diplonemids in deep-sea pelagic waters, notably the deep sea pelagic diplonemids clade I and II (DSPD I, II) (Lara *et al*., 2009). In a comprehensive marine survey, diplonemids emerged even as the 3rd most diverse and 6th most abundant group of oceanic eukaryotes (de Vargas *et al*., 2015; Lukeš *et al*., 2015) populating virtually all stations and all depths examined in the comprehensive *Tara* Oceans expedition (de Vargas *et al*., 2015; Flegontova *et al*., 2016). Analysis of the V9 18S rRNA sequence suggests that diplonemids may even be the most species-rich among all marine eukaryotes (Flegontova *et al*., 2016). At present, only diplonemids from the *Diplonema/*

*Rhynchopus* (*D/R*) clade can be grown axenically and are available from the American Type Culture Collection (ATCC). Representatives of the hyper-diverse DSPD clades are not yet in culture. An initial examination of 10 DSPD isolates has been performed by single-cell genomics (Gawryluk *et al*., 2016).

Among the common structural features of diplonemids is their sac-like shape with cell sizes ranging from 5 to 50 μm, their highly metabolic movement, and the presence of two sub-apical flagella. They possess a single mitochondrial network lining the inside of the plasma membrane and containing a large amount of mitochondrial DNA (mtDNA) (Marande *et al*., 2005). Whether diplonemids have a parasitic, commensal, or free-living life-style is still an open question. Hence the ecological role of diplonemids in the oceanic ecosystem remains elusive (Lukeš *et al*., 2015). This important gap in knowledge reflects our ignorance about the ecological functions of marine protists in general (Worden and Wilken, 2016), and the lack of a suitable model system for diplonemids in particular.

Establishing a model organism requires several crucial steps to be fulfilled, the most prominent being their availability in culture, and the ability to genetically modify the species. Ideally, a genetic system includes a vector, a transformation system, and a selectable marker, all of which facilitate expression of introduced genes, including transcription, post-transcriptional processing, and translation. All these steps require extensive experimentation and optimization for each target organism, but once a protocol established, it is generally straightforward to create any range of constructs to address many functional questions.

Only a single diplonemid species, *Diplonema papillatum*, has been examined at the molecular level in much detail. *D. papillatum* is a free-living protist with two short heterodynamic flagella that was first isolated from seawater at Friday Harbor, Washington (Porter, 1973). This species is available from the American Type Culture Collection (ATCC), can be easily cultivated axenically in the laboratory at high cell densities, and can be cryopreserved. The mitochondrial genome and transcriptome have been analyzed in detail, revealing novel modes of post-transcriptional gene expression (Marande and Burger, 2007; Kiethega *et al*., 2013; Moreira *et al*., 2016; Valach *et al*., 2016; Faktorová *et al*., 2018). Further, *D. papillatum* has been investigated regarding its compartmentalization of gluconeogenesis (Makiuchi *et al*., 2011; Morales *et al*., 2016). Finally, the nuclear genome has recently been sequenced and assembled, and functional annotation is under way (unpubl. data).

For all these reasons, establishing a tractable genetic system for *D. papillatum* and establishing it as a model system would be highly desirable. Here, we describe all key steps necessary for genetic manipulation of this marine flagellate.

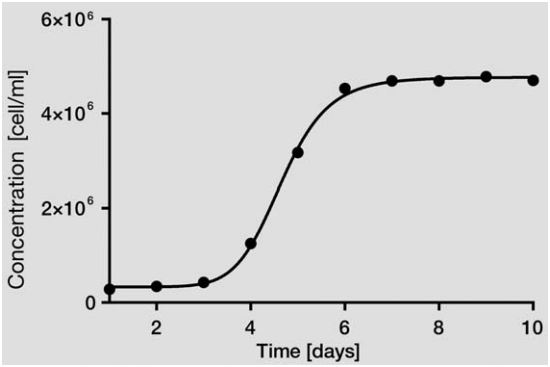


**Fig. 1.** The growth curve of *D. papillatum* cells during 10 days in *Diplonema* cultivation medium. Inoculation titer at time 0 was $2 \times 10^5$ cells/ml.

## Results

### *Optimization of cultivation and electroporation conditions*

In the standard seawater medium (see Experimental Procedures), *D. papillatum* cultures reach the exponential phase at a cell density of 2–4 $\times$ $10^6$ cells/ml. The highest cell density obtained is 6 $\times$ $10^6$ cells/ml with a doubling time of 12 h (Fig. 1).

To introduce foreign DNA into *D. papillatum*, we first tested electroporation as the technique of choice, as it is being successfully and extensively used for transforming *Trypanosoma brucei* and several other trypanosomatids (Beverley and Clayton, 1993). Since diplonemids and trypanosomatids are closely related and share a number of fine-structural features including a corset of subpellicular microtubules (Roy *et al*., 2007; Tashyreva *et al*., 2018), we reasoned that electroporation may also be suitable for *D. papillatum*.

As a first step, we confirmed that *D. papillatum* cells survive for at least 10 min in electroporation buffers (Cytomix - used for BTX electroporator or Amaxa - used for Amaxa Nucleofector II) and thus can be electroporated in standard electroporation buffers. Survival rate was $>$ 90%. Next, two different electroporation apparatuses were tested: BTX electroporator and Amaxa Nucleofector II (see Experimental Procedures), for which we optimized several parameters, such as the composition of electroporation buffer, the electroporation program, and the amount of DNA used for transformation (Table 1). Specifically, cells were pelleted by a short centrifugation, re-suspended in electroporation buffer, subjected to the electric pulse, transferred back into seawater-containing medium, and then observed under the microscope. While electroporation with BTX killed the majority of cells, the Amaxa procedures yielded more than 20% survival (see Table 1), with cells retaining their original shape, and demonstrating full recovery after a few hours. The Amaxa Nucleofector II

**Table 1.** Used electroporation programs and survival rate of *D. papillatum* cells.

| Electroporation machine | Used program | Survival rate |
|---|---|---|
| BTX | 1600V, 25Ω, 50 μF | 10% |
| Amaxa Nucleofector II | preset program X-001 | 50%-60% |
| Amaxa Nucleofector II | preset program X-014 | 20%-30% |

programs proved to be best suited and therefore were chosen for further experiments (Table 1).

### *Identification of selectable markers*

To identify selection markers, we tested the sensitivity of *D. papillatum* to seven antibiotics—hygromycin, geneticin, phleomycin, puromycin, blasticidin, nourseothricin and tetracycline. With the exception of tetracycline, these drugs have been extensively used for genetic manipulation of *T. brucei* and related trypanosomatids (http://tryps.rockefeller.edu/). The antibiotic concentration for selection of *D. papillatum* transformants was assessed by determining cell viability by the Alamar Blue assay (Räz *et al*., 1997).

*Diplonema papillatum* was found to be sensitive to all the selection markers tested, except tetracycline. The effective concentrations for selection of electroporated *D. papillatum* are shown in Fig. 2 and Table 2**.**

The highest antibiotic sensitivity of *Diplonema* is to puromycin.

### *Rationale for construct design for* Diplonema *transformation*

Our overall strategy for transformation is to incorporate foreign DNA via genomic integration, since nothing is known about DNA replication in this group and no native plasmids are known. Due to the high number of repetitive regions in the nuclear genome sequence of *D. papillatum* (unpubl. data), we restricted our selection of genomic regions to target for integration to genes that met several criteria. The genes must (i) be contained inside validated genomic contigs and (ii) be intron-less. Further the corresponding

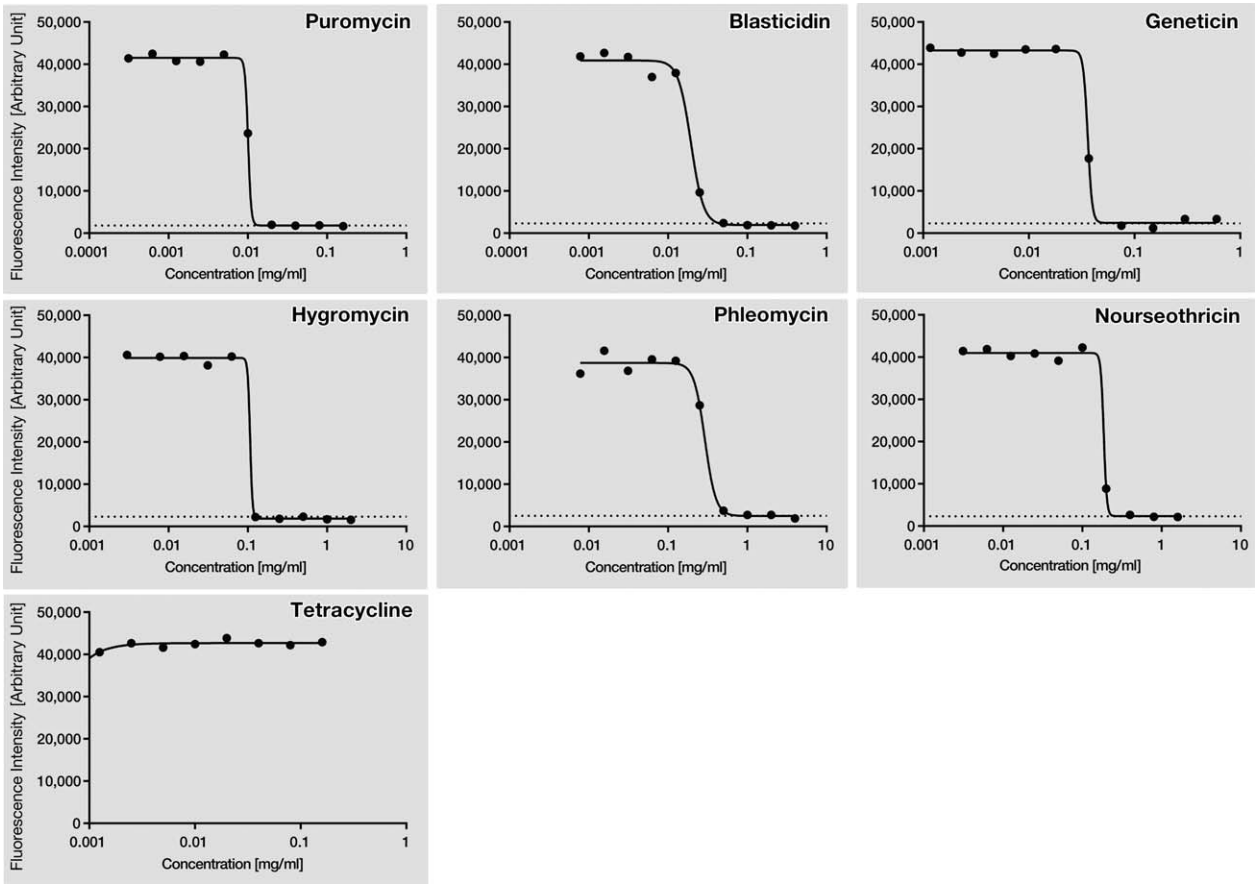


**Fig. 2.** Antibiotic sensitivity of *D. papillatum*. Effect of various concentrations of antibiotics (mg/ml; *x* axis) on survival of *Diplonema* cells, as determined by the Alamar blue assay, which measures viability by fluorescence (see Experimental Procedures). The fluorescence intensity corresponding to 1% cell survival is indicated by a dotted horizontal line.

**Table 2.** Tested resistance markers and their concentration used for selection.

| Antibiotic | Concentration (μg/ml) |
|---|---|
| Puromycin | 20 |
| Blasticidin | 50 |
| Geneticin | 75 |
| Hygromycin | 125 |
| Nourseothricin | 400 |
| Phleomycin | 500 |
| Tetracycline | not sensitive |

mRNAs must (iii) have a high steady state level (rank among the top hundred by their expression level) and (iv) carry a spliced leader (SL) at their 5′ end (Sturm *et al*., 2001).

In order to confirm proper integration, the target gene was tagged with a cassette that is composed of a fluorescent protein tag and a resistance gene, both flanked by 5′ and 3′ UTRs from *Diplonema*. To direct the integration of this cassette into the proper genomic position via homologous recombination, we appended to the cassette appropriate sequences of *D. papillatum* genome (targeting regions). This strategy, successfully used in numerous model systems (Stretton *et al*., 1998; Janke *et al*., 2004; Lai *et al*., 2010; Wang *et al*. 2017), should lead to antibiotic-resistant transformants expressing a fluorescently labelled protein that can be detected with a fluorescent microscope or by commercially available antibodies.

### *Endogenous N-terminal tagging of α-tubulin*

Based on the above described strategy, we have designed a construct for tagging the N-terminus of the *Diplonema* α-tubulin gene. The cassette contains the puromycin resistance gene (*pac*), here called puromycin$^R$ (encoding the puromycin N-acetyltransferase of *Streptomyces alboniger*), which from all tested drugs was selectable at the lowest concentrations (Table 2). Moreover, it also contains the sequence encoding the fluorescent protein mCherry which lacks the stop codon, as we intended to create a fused mCherry-α-tubulin protein. We chose mCherry, which emits red light, to avoid overlap with the quite strong green autofluorescence of *D. papillatum* (our unpubl. data). The puromycin$^R$-mCherry cassette (∼ 2 kbp) was flanked by *D. papillatum* sequences including 5′ and 3′ UTRs and homology regions about 500 bp long, which ought to enhance the integration of the construct into the targeted locus. A schematic representation of this construct is shown in Fig. 3A. A similar tagging approach was recently used for cytoskeleton studies in *T. brucei* (Sheriff *et al*., 2014).

### *Transfection of* Diplonema *leads to stable chromosomal integration of foreign DNA*

Both *Not*I-linearized and circular constructs were then electroporated into *Diplonema* cells in parallel and the transfectants were subjected to selection with increasing concentrations of puromycin to ensure stringent selection.

A total of 10 puromycin-resistant *Diplonema* clones were recovered after 8–10 days, at which time point a negative-control culture represented by wild type cells without the construct and in the presence of the drug did not display any viable cells.

Clones A3 and A4 (labelled according to their position in the 24-well plate) were investigated in detail by PCR and amplicon sequencing showing the presence of the puromycin$^R$-mCherry cassette in *Diplonema* genomic DNA (Fig. 3B; Supporting Information Figs. S1 and S4). To verify the cassette's presence in the genome, we performed Southern blot analysis using radioactively labelled probes against mCherry (Fig. 3**C**). The expected size of the *Spe*I-*Nde*I restriction fragment containing the mCherry CDS is 1969 bp, which corresponds to the detected band size (Fig. 3**C**, right). Digestion of genomic DNA with *Pci*I should produce a fragment of 9699 bp in case the cassette has integrated into the expected site by homologous recombination; however, we detected bands of ∼ 3.5 kbp (Fig. 3**C**, left). We, therefore, conclude that the complete cassette has been incorporated in the two *D. papillatum* transformants, but at heterologous sites in the genome. In line with this observation, amplification of the cassette with primers outside the cassette failed (data not shown).

### *Introduced heterologous gene can be transcribed, post-transcriptionally processed and translated in* Diplonema

To examine whether mCherry and puromycin$^R$ are transcribed in the *D. papillatum* transformants A3 and A4, we conducted reverse transcription followed by PCR amplification of the first-strand cDNA (RT-PCR). This experiment produced a single band of expected size confirming transcription of the two heterologous genes (Fig. 4B; Supporting Information Fig. S5A). We also confirmed, by nested RT-PCR, that the mCherry and puromycin$^R$ mRNAs are properly processed post-transcriptionally by addition of the SL RNA to their 5′ end (Fig. 4C; Supporting Information Figs. S2 and S5B).

To verify translation of the heterologous genes in A3 and A4 clones, we checked mCherry fluorescence and performed Western blots with an anti-mCherry antibody. However, in both cases no signal was detected, as expected due to the integration of the cassette into a different site. In contrast, translation of the puromycin$^R$ gene could be demonstrated by two different immunoassays,

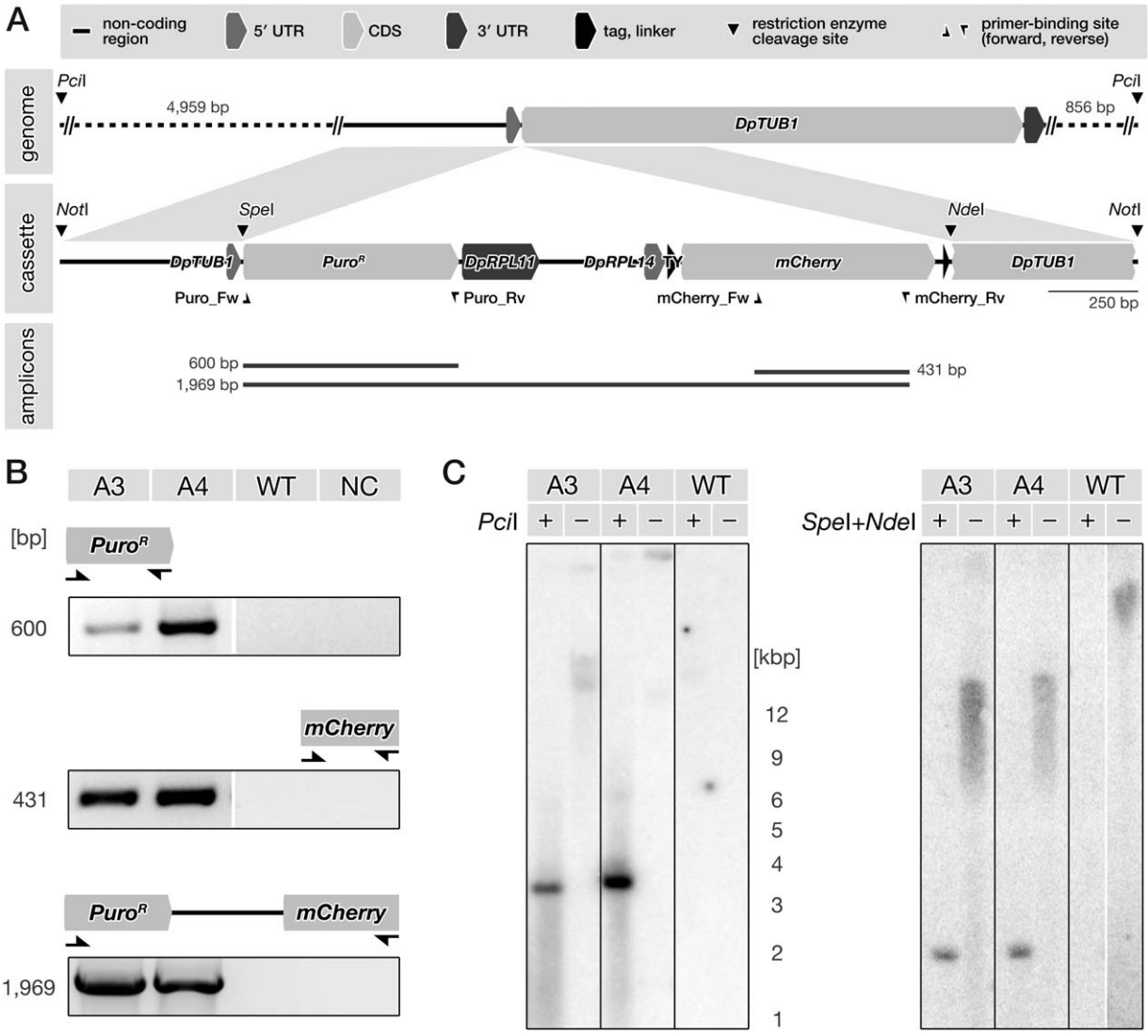


**Fig. 3.** Confirmation that the electroporated construct is integrated in the *D. papillatum* genome.
A. Scheme of the puromycin$^R$ (puro$^R$) + mCherry cassette (2995 bp *Not*I fragment) including restriction sites, positions of the primers and expected sizes of the amplicons.
B. PCR of total DNA of *D. papillatum* wild type (WT) and selected transformants (A3 and A4) using specific primers for amplification of puromycin$^R$ and mCherry CDSs. Negative control PCR (NC) was performed without template DNA. The explicit sequences are shown in Supporting Information Fig. S1 and the whole gels are shown in Supporting Information Fig. S4.
C. Southern hybridization of total DNA from *D. papillatum* wild type (WT) and transformants A3 and A4 using a DNA fragment of mCherry as a radiolabelled probe. Right panel, total DNA digested with *Spe*I+*Nde*I, which cut inside the cassette (+), and undigested (-). The *Spe*I+ *Nde*I band is of expected size—1969 bp. Left panel, total DNA digested *Pci*I, which cuts outside the cassette (+), and undigested (-). In case of homologous integration, the expected size of the *Pci*I band is 9699 bp, however, we detected bands of ~ 3.5 kbp.

one using the anti-Puromycin antibody, and the other using the anti-Puromycin N-acetyltransferase antibody.

Puromycin is an aminonucleoside antibiotic that functions as an inhibitor of protein synthesis by disrupting peptide transfer on ribosomes, causing premature chain termination during translation. Since its structure resembles the 3′ end of aminoacylated tRNA, puromycin enters the acceptor site of the ribosome and is added to the growing polypeptide chain, which leads to premature termination of the newly synthesized proteins (Pestka, 1971). Anti-Puromycin antibody binds puromycin-containing newly synthesized proteins, visible in Western blot as a smear due to their different molecular weights. *Diplonema* wild type cells show indeed a strong signal of a broad molecular weight range, while the A3 and A4 clones do not (Supporting Information Fig. S3). This indicates that puromycin is not incorporated in the proteins of the clones A3 and A4, providing indirect evidence for the translation

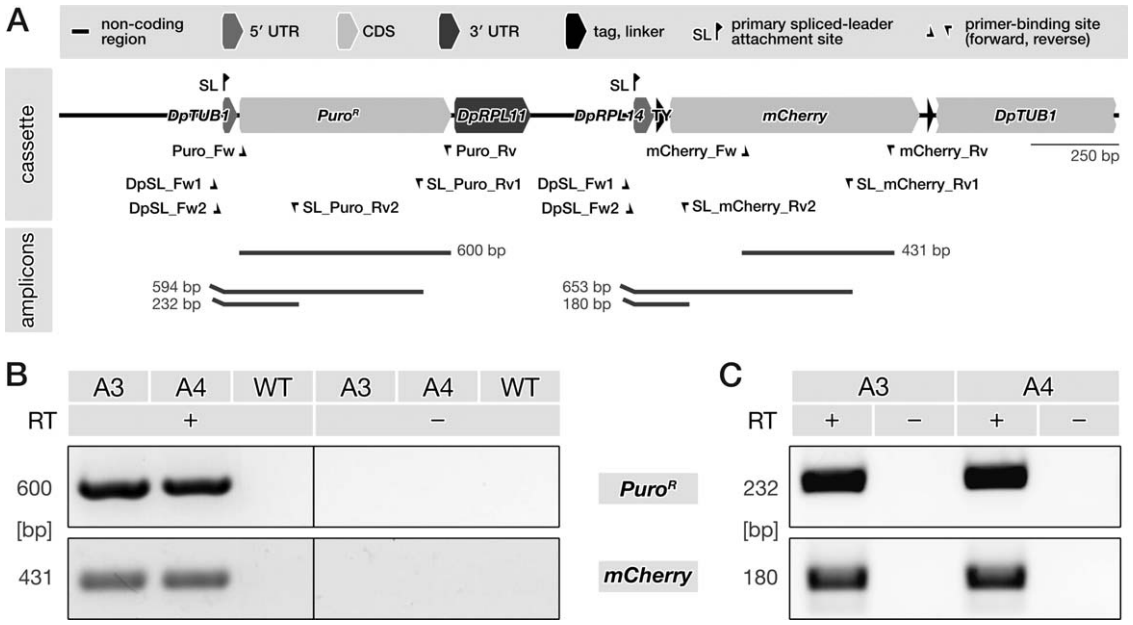


**Fig. 4.** Validation of proper transcription and post-transcriptional 5′ end-processing of the transcripts produced from heterologous genes in *D. papillatum*.
A. Scheme of the puromycin$^R$ (puro$^R$) + mCherry cassette including positions of the spliced leader (SL) primers and expected sizes of the amplicons of 5′ region from the puromycin$^R$ transcript and the mCherry transcript. RT-PCR primers used for amplifying mCherry and puromycin$^R$ (puro$^R$) cDNAs are the same as shown in Fig. 3B.
B. Demonstration that heterologous genes in *D. papillatum* are transcribed. RNA from *D. papillatum* wild type (WT) and transformants A3 and A4 was used as a template for RT-PCR. Expected sizes of the RT-PCR products are indicated. Reactions with reverse transcriptase added and negative controls without reverse transcriptase are indicated by (+) and (-). The whole gels are shown in Supporting Information Fig. S5A.
C. The amplification of the 5′ region from the puromycin$^R$ (puro$^R$) transcript and the mCherry transcript respectively. Nested SL RT-PCR using total RNA from the transformants A3 and A4 as templates, and two sets of primers that anneal to the conserved SL sequence of *D. papillatum* (forward primers) and to the 5′ end of the transcripts (reverse primers). The explicit sequences are shown in Supporting Information Fig. S2 and the whole gels are shown in Supporting Information Fig. S5B.

of the puromycin$^R$ gene in the transformants (Supporting Information Fig. S3).

Similarly, Western immunoassays with the anti-Puromycin N-acetyltransferase antibody show clear expression of the heterologous puromycin$^R$ gene in A3 and A4, revealing distinct bands of the expected size (Fig. 5; Supporting Information Fig. S6). In both experiments, puromycin-resistant and sensitive cell lines from *T. brucei* served as negative and positive controls.

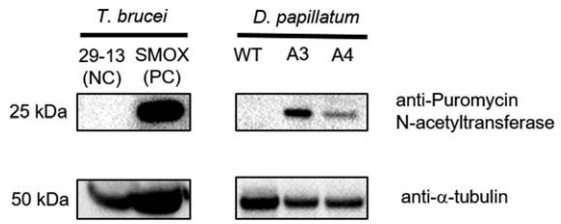


**Fig. 5.** Western blot analysis of *D. papillatum* wild type (WT) and of transformants A3 and A4 that express the puromycin$^R$ gene (puromycin N-acetyltransferase).
Monoclonal rabbit anti-Puromycin N-acetyltransferase antibodies (1:500) and secondary anti-rabbit antibodies coupled to horseradish peroxidase (1:1000). 29-13, *T. brucei* procyclic-stage cell line 29-13, which does not express the puromycin$^R$ gene, is used as a negative control (NC). SMOX, *T. brucei* cell line SMOX P9, which does express the puromycin$^R$ gene, is used as a positive control (PC). Anti-α-tubulin antibodies were used as a loading control. The whole gels are shown in Supporting Information Fig. S6.

## Discussion

Very few marine protists have been successfully transformed at present, most notably members of the green and red microalgae, diatoms, chlorarachniophytes (for review see Gong *et al*., 2011), and further the alveolate *Perkinsus marinus* (Fernández-Robledo *et al*., 2008), the prasinophyte *Ostreococcus tauri* (van Ooijen *et al*., 2012), the haptophyte *Pleurochrysis carterae* (Endo *et al*., 2016) and recently the kinetoplastid *Parabodo caudatus* (Gomaa *et al*., 2017). Different transfection methods were used, notably polyethylene glycol-mediated approach for the haptophyte, otherwise microprojectile bombardment or electroporation.

### *The challenge of electroporating marine organisms*

Electroporation induces a transient destabilization of the cell membrane, which then becomes highly permeable to

foreign DNA, proteins or small molecules. Electroporation is used particularly for suspension cultures as all cells are essentially transfected simultaneously (Heiser, 2000). For transforming *D. papillatum*, we have opted for electroporation, which is an established technique in kinetoplastids, the sister group of diplonemids (e.g., Adl *et al.*, 2012), specifically in the medically important *Trypanosoma* and *Leishmania* (Beverley and Clayton, 1993).

The technical challenge of electroporating marine organisms is that salts in the medium cause electrical discharge (arcing), which reduces the viability of the organism (Potter and Heller, 2003). In the case of *Parabodo caudatus* (Gomaa *et al.*, 2017), electroporation succeeded because this microeukaryote lives in both freshwater and marine environments and is, therefore, only moderate sensitive to low salt concentrations. Fortunately, *D. papillatum* is also tolerant to brackish water, and thus endures short-term exposure to the low-salt electroporation buffer.

### *Integration and expression of heterologous genes in the* Diplonema *nucleus*

For two transformed *D. papillatum* clones, we demonstrated by PCR, DNA sequencing, and Southern blot analysis that the transfection constructs are readily integrated into the nuclear genome. However, the constructs integrated at apparently random genomic positions, a common issue in many genetic systems including mammalian and plant systems (Sargent *et al.*, 1997; Gorbunova and Levy, 1999). Ectopic integration may be due to the fact that the genome of *Diplonema* is highly repetitive, or, alternatively, because homologous recombination (HR) may be less efficient in this organism than microhomology-mediated end-joining (MMEJ) or the classical non-homologous end-joining (NHEJ) DNA repair/recombination pathways (for a review see Michael, 2010). Note that the genes known to be involved in the corresponding machineries are present in the *D. papillatum* genome (our unpubl. data).

Importantly, however, transfected heterologous genes are nevertheless expressed in *Diplonema*. The protein tag (mCherry) and resistance gene (puromycin$^R$) used here are transcribed, and the SL is correctly *trans*-spliced onto the 5′ end of the transcripts. For the puromycin$^R$ gene, we were able to demonstrate translation into protein and observe the expected resistant phenotype. In contrast, translation of the mCherry transcript was neither observed nor expected, because a stop codon and a 3′ UTR were absent, as it was designed to be fused to the $\alpha$-tubulin gene as an N-terminal tag. Due to the lack of a stop codon and/or poly-(A) tail, the mRNA may have been degraded by one of the quality control mechanisms of the eukaryotic cell (Klauer and van Hoof, 2012).

Since the purpose of this construct was to create a fused protein composed of N-terminally tagged $\alpha$-tubulin with mCherry, the stop codon at the end of the mCherry gene was intentionally removed. However, as this construct was not integrated into a proper position, no expression of mCherry could be observed.

An alternative approach to obtain resistant cell line emitting red fluorescence would be to design a cassette containing intact genes and corresponding UTRs to replace an endogenous gene such as tubulin, or insert the cassette into a particular position in the *Diplonema* genome, f.e. in a transcriptionally silent region, a routinely strategy in other organisms. While this approach would not produce a labelled endogenous protein, it would allow the expression of the mCherry protein. In our future work, we will apply different strategies with the aim to achieve correct integration of the cassette.

### *Future prospects for* D. papillatum *as a genetic system*

Taken together, these data show that *D. papillatum* has all prerequisites for becoming a genetically tractable organism. Successful transformation provides first example of heterologous gene expression in an euglenozoan protist outside the kinetoplastids, and raises questions about how widely these methods can be applied within the group, and what other tools can now be used in model diplonemids. Currently, only half a dozen diplonemids are available in the ATCC collection and can be cultivated in the laboratory. For the time being, with a representative of the species-rich DSPD I clade yet to be brought into culture, the next candidate for transformation is *Hemistasia phaeocysticola* (Yabuki and Tame, 2015; Yabuki *et al.*, 2016), which is more closely related to the most abundant diplonemids. However, this species is also much more challenging to work with, as it prefers live diatoms as a food source, reaches only low cell densities and so far could not be cryopreserved (our unpubl. data).

The availability of a methodology to transfect *Diplonema* will also facilitate investigation of the machineries that drive the unique post-transcriptional processes in their mitochondria, such as U-appendage RNA editing and *trans*-splicing of fragmented genes (for reviews see Valach *et al.*, 2016; Faktorová *et al.*, 2018). For example, fluorescence tagging of terminal uridyl transferases or RNA ligases would identify the respective enzyme that acts in mitochondria, and open the venue for uncovering other components in the hypothetical editosome or trans-spliceosome.

Future work may achieve targeted integration by further extension of the 5′ and 3′ homologous regions of the constructs to more than 1500 bp, as shown in trypanosomes (Barnes and McCulloch, 2007). Furthermore, it would be worthwhile to explore the CRISPR/Cas9 strategy, which was recently successfully implemented in kinetoplastids (Lander *et al.*, 2016; Beneke *et al.*, 2017). In this strategy, a circular plasmid that is in the transformed organism

retained either as an episome or as a linearized plasmid, or a PCR product containing homologous targeting regions for genome integration can be used. For *Diplonema*, PCR amplicons are of higher priority, as attempts to maintain circular plasmids as non-integrated episomes have failed thus far. Last, but not least, we will also try to enhance the efficiency of the homologous recombination pathway using inhibitors of the non-homologous end joining pathway, as recently described in *Cryptococcus neoformans* (Arras *et al.*, 2016). As a high quality genome and transcriptome of *D. papillatum* shall soon be available, it would be beneficial to have a transformation protocol in place. We envisage its application in functional analysis of proteins with potential ecological significance, such as those involved in pathways that respond to environmental stress.

## Experimental procedures

### *Strains, cultivation and growth curves*

*D. papillatum* (ATCC 50162) was cultivated axenically at 27°C in an artificial sea salt mixture 40 g/l (Sigma, S9883), 0.1% (w/v) tryptone, 1% (v/v) fetal bovine serum and 100 μg/ml of chloramphenicol. Cell density was measured manually by the Neubauer cell chamber. Before measurement, cells had to be fixed in 3.7% (v/v) formaldehyde in SSC to retain their shape and to prevent them from moving prior to counting.

### *Determination of resistance to antibiotics using Alamar Blue assay*

The inhibition concentration where 99% of the cell population is dead (IC99) was determined using the fluorescence viability indicator Alamar blue (Resazurin sodium salt, Sigma, R7017) as described in Gould *et al.* (2013). It is based on resazurin, a non-toxic, permeable and weakly fluorescent dye used as a redox indicator. Its reduced form or resorufin is pink and highly fluorescent, with its fluorescence intensity being proportional to the number of respiring (e.g., metabolically active) cells. Cells were inoculated into the 96-well flat-bottomed microtiter plate (Costar) at a concentration $1 \times 10^5$ cells/ml. Seven drugs (hygromycin, puromycin, phleomycin, geneticin, blasticidin, nourseothricin and tetracycline) were tested in triplicates using serial dilutions at 27°C for 48 h; wells without the drug at the end of each row were used as a control. Resazurin was prepared at a concentration of 0.125 mg/ml in PBS and added to the plate after 48 h of incubation with the drugs. The plate was subsequently incubated for another 24 h and fluorescence was read at 585 nm using a Tecan Infinite M200. Data were analyzed using Prism 5.0 software (GraphPad, San Diego, CA) and IC99 values were derived from sigmoidal dose-response curves with variable slopes.

### *Design and preparation of transformation cassette*

Design of the puromycin$^R$ + mCherry cassette (Fig. 3**A**) was performed using the UTRs from the *D. papillatum* genome to drive the expression. The entirely modular cassette (2996 bp-long) was designed for the N-terminal tagging and contained the following fragments ordered in the 5′–3′ direction, starting with a *Not*I restriction site: 499 nt of the sequence just before the beginning of α-tubulin gene *DpTUB1* including its 5′UTR, puromycin N-acetyltransferase gene (puromycin$^R$) with the stop codon, 3′ UTR of *DpRPL11*, 5′ UTR of *DpRPL14*, a TY tag and the mCherry CDS without the stop codon followed by a linker, 510 nt of the 5′ of the α-tubulin gene *DpTUB1*, followed by a second *Not*I site. The cassette was synthesized by Biomatik (http://www.biomatik.com), cloned into pBluescript II SK(+) vector and the sequence was submitted to GenBank (Acc. No. MG490656).The vector was isolated using QIAprep Spin Miniprep Kit (Qiagen, 27106) and either directly used for electroporation or cut with *Not*I restriction enzyme, isolated from the gel using QIAquick Gel Extraction Kit (Qiagen, 28706), and re-suspended in 10 μl of deionized distilled water before electroporation.

### *Electroporation and obtaining of the transformants*

A total of $5 \times 10^7$ cells ($2 \times 10^6$ cells/ml) was harvested by centrifugation at 1300 g for 10 min at 25°C and re-suspended either in 100 μl cytomix buffer (van den Hoff *et al.*, 1992) and electroporated with the BTX machine (1600V, 25Ω, 50 μF), or in 100 μl of AMAXA buffer (81.8 μl of Human T-cell nucleofector solution + 18.2 μl of Supplement) for the electroporation by Amaxa Nucleofector II.

Ten to 15 μg of DNA were mixed with electroporation buffer and *Diplonema* cells before transferring into the electroporation cuvette and electroporation. After the electroporation pulse was applied to the cuvette, the mixture was immediatelly transferred into 10 ml of *Diplonema* growth media. Subsequently, the cells were allowed to recover for about 8 h and the transfectants were subjected to selection with increasing concentrations (12–40 μg/ml) of puromycin. While this wide range makes the experiment more time consuming, it ensured stringent selection of transformants. Clones A3 and A4 examinated in details were cultivated in 24 and 28 μg/ml of puromycin, respectively.

Following an expansion of each clone to a volume of 20 ml transformants had been cultured for up to 8 weeks prior to testing by PCR, which proved that all of them indeed contain integrated constructs. We were able to freeze-store the transformants in 10% glycerol-containing medium at −80°C or in liquid nitrogen for several months.

### *PCR using genomic DNA*

Genomic DNA was isolated using Qiagen DNA isolation kit (Qiagen, 69504). Primer pairs used for verification of the integration are shown in Fig. 3A, for primer sequences see Supporting Information Table S1. PCR amplification was done using OneTaq polymerase (NEB Biolabs, M0486L) and the following program: initial denaturation 94°C for 3 min, denaturation at 94°C for 30 s, annealing at 58°C for 60 s, extension at 68°C for 3 min and a final extension at 68°C for 10 min, for 30 cycles. To amplify mCherry and puromycin$^R$, a lower extension of 68°C for 1 min 30 s and a final extension of 68°C for 5 min were used. Cassette integration in the genome of *D. papillatum* was confirmed by sequencing of the PCR products (Eurofins Genomics).

### *Southern blot hybridization*

Southern blot analysis was performed as previously described (Lai *et al*., 2008). Total DNA was isolated from wild type cells and transformed clones, digested with selected restriction enzymes and subjected to agarose gel electrophoresis. Samples were blotted overnight to a Zeta-Probe membrane (Bio-rad) by capillarity and subsequently cross-linked with UV light as described (Vondrušková *et al*., 2005). The mCherry probe was PCR amplified using mCherry_Fw and mCherry_Rv primers and radiolabelled with [$\alpha$–$^{32}$P]dATP using Radioactive DNA Labelling kit (Thermo Scientific DecaLabel DNA Labelling Kit, #K0622) and hybridization with the probe was performed overnight at 60°C according to the Zeta-Probe membrane manual. The membrane was exposed to a Fuji Imaging phosphor screen (28956475, BAS-MS 2025) and scanned in a Phosphoimager (Amersham, GE Healthcare, Typhoon 9400) for signal detection.

### *RNA isolation and cDNA synthesis, RT-PCR and SL RNA-PCR*

Total RNA was isolated using TriReagent (MRC, TR118) and pellet was re-suspended in 30 $\mu$l of RNAse-free water. cDNA was prepared using QuantiTect Reverse Transcription Kit (Qiagen, 205311) with random primers. PCR was performed on cDNA with primers shown in Fig. 3A (for primer sequences, see Supporting Information Table S1), and OneTaq polymerase (NEB Biolabs, M0486L), with the following protocol: 30 s at 94°C; 30 cycles of 30 s at 94°C, 30 s at 60°C and 1 min 30 s at 68°C, and a final extension for 5 min at 68°C. The same reactions without reverse transcriptase (RT-) were used as negative controls.

The cDNA was used as a template for nested PCR with the following program: 30 s at 94°C; 30 cycles of 30 s at 94°C, 30 s at 58°C and 1 min 30 s at 68°C, followed by a final extension (5 min at 68°C). DpSL_Fw1 and DpSL_Fw2 primers derived from the SL RNA gene were used in combination with mCherry (SL_mCherry_Rv1; SL_mCherry_Rv2) or puromycin$^R$ specific primers (SL_Puro_Rv1; SL_Puro_Rv2; Supporting Information Table S1). The position of primers and expected size of PCR products is shown in Fig. 5. An amplicon containing the SL and N-terminus of puromycin$^R$ or mCherry was obtained and verified by sequencing (Eurofins Genomics; Supporting Information Fig. S2).

### *Western blot*

Cell lysates were prepared in 2× SDS sample buffer using 1 × $10^7$ cells per lane and separated on a 12% (v/v) SDS-PAGE gel and proteins were subsequently transferred onto the PVDF membrane by electroblotting. Membranes were blocked overnight with 5% (w/v) non-fat milk prepared in PBS 0.5% (v/v) Tween 20 and probed with the primary monoclonal mouse anti-Puromycin antibody (1:500) (Merck, MABE343) overnight at 4°C. The membrane was subsequently incubated with the secondary anti-mouse polyclonal antibody conjugated with horseradish peroxidase (1:1000) (Sigma) and visualized using Clarity western ECL substrate (Bio-Rad).

For the detection of puromycin N-acetyltransferase (*pac* gene product), cell lysates were prepared in NuPAGE LDS sample buffer (Invitrogen) using 1 × $10^7$ cells per lane separated on Bolt 4%–12% Bis-Tris polyacrylamide gels (Invitrogen) and transferred to a Amersham Hybond P PVDF membrane (GE Healthcare), blocked overnight with 5% (w/v) non-fat milk prepared in PBS 0.5% (v/v) Tween-20 and subsequently hybridized with the primary monoclonal rabbit anti-Puromycin N-acetyltransferase antibody (1:500) (ThermoFisher Scientific) and subsequently with secondary anti-rabbit polyclonal antibody coupled to horseradish peroxidase (1:1000). Monoclonal anti-$\alpha$-Tubulin antibody produced in mouse (1:1000) (Sigma, T9026) was used as a loading control.

## Acknowledgements

We thank Jorge Morales (Heinrich Heine University Düsseldorf) for discussion in the initial stages of the project; Anzhelika Butenko and Pavel Flegontov (Institute of Parasitology) for help with the selection of genes and design of the constructs; Galina Prokopchuk and Daria Tashyreva (Institute of Parasitology) for sharing unpublished data. Support from the Grant Agency of University of South Bohemia (050/2016/P to BK), the Czech Grant Agency (15–21974S and 16–18699S to JL), the ERC CZ (LL1601 to JL), the Canadian Institute of Health Research (CIHR, MOP 70309 to GB) and from the Gordon and Betty Moore Foundation (GBMF4983.01 to JL, GB and PK) are kindly acknowledged.

## Conflict of Interest

Authors have no conflict of interest to declare.

## References

Adl, S.M., Simpson, A.G.B., Lane, C.E., Lukeš, J., Bass, D., Bowser, S.S., *et al*. (2012) The revised classification of eukaryotes. *J Eukaryot Microbiol* **59:** 429–493.

Arras, S.D.M., Fraser, J.A., and Lustig, A.J. (2016) Chemical inhibitors of non-homologous end joining increase targeted construct integration in *Cryptococcus neoformans*. *PLoS One* **11:** e0163049.

Barnes, R.L., and McCulloch, R. (2007) *Trypanosoma brucei* homologous recombination is dependent on substrate length and homology, though displays a differential dependence on mismatch repair as substrate length decreases. *Nucleic Acids Res* **35:** 3478–3493.

Beneke, T., Madden, R., Makin, L., Valli, J., Sunter, J., and Gluenz, E. (2017) A CRISPR Cas9 high-throughput genome editing toolkit for kinetoplastids. *R Soc Open Sci* **4:** 170095.

Beverley, S.M., and Clayton, C.E. (1993) Transfection of *Leishmania* and *Trypanosoma brucei* by electroporation. *Methods Mol Biol* **21:** 333–348.

Breglia, S.A., Yubuki, N., Hoppenrath, M., and Leander, B.S. (2010) Ultrastructure and molecular phylogenetic position of a novel euglenozoan with extrusive episymbiotic bacteria: *Bihospites bacati* n. gen. et sp. (Symbiontida). *BMC Microbiol* **10:** 145.

de Vargas, C., Audic, S., Henry, N., Decelle, J., Mahe, F., Logares, R., *et al*. (2015) Eukaryotic plankton diversity in the sunlit global ocean. *Science* **348:** 1261605.

Endo, H., Yoshida, M., Uji, T., Saga, N., Inoue, K., and Nagasawa, H. (2016) Stable nuclear transformation system for the coccolithophorid alga *Pleurochrysis carterae*. *Sci Rep* **6:** 22252.

Faktorová, D., Valach, M., Kaur, B., Burger, G., and Lukeš, J. (2018) Mitochondrial RNA editing and processing in diplonemid protists. "RNA Metabolism in Mitochondria", Springer series "Nucleic Acids and Molecular Biology", in press.

Fernández-Robledo, J.A., Lin, Z., and Vasta, G.R. (2008) Transfection of the protozoan parasite *Perkinsus marinus*. *Mol Biochem Parasitol* **157:** 44–53.

Flegontova, O., Flegontov, P., Malviya, S., Audic, S., Wincker, P., de Vargas, C., *et al*. (2016) Extreme diversity of diplonemid eukaryotes in the ocean. *Curr Biol* **26:** 3060–3065.

Gawryluk, R.M.R., del Campo, J., Okamoto, N., Strassert, J.F.H., Lukeš, J., Richards, T.A., *et al*. (2016) Morphological identification and single-cell genomics of marine diplonemids. *Curr Biol* **26:** 3053–3059.

Gong, Y., Hu, H., Gao, Y., Xu, X., and Gao, H. (2011) Microalgae as platforms for production of recombinant proteins and valuable compounds: progress and prospects. *J Ind Microbiol Biotechnol* **38:** 1879–1890.

Gomaa, F., Garcia, P.A., Delaney, J., Girguis, P.R., Buie, C.R., and Edgcomb, V.P. (2017) Toward establishing model organisms for marine protists: successful transfection protocols for *Parabodo caudatus* (Kinetoplastida: Excavata). *Environ Microbiol* **19:** 3487–3499.

Gorbunova, V.V., and Levy, A.A. (1999) How plants make ends meet: DNA double-strand break repair. *Trends Plant Sci* **4:** 263–269.

Gould, M.K., Bachmaier, S., Ali, J.A., Alsford, S., Tagoe, D.N., Munday, J.C., *et al*. (2013) Cyclic AMP effectors in African trypanosomes revealed by genome-scale RNA interference library screening for resistance to the phosphodiesterase inhibitor CpdA. *Antimicrob Agents Chemother* **57:** 4882–4893.

Griessman, K. (1914) Ueber marine Flagellaten. *Arch Protistenkd* **32:** 1–78.

Heiser, W.C. (2000) Optimizing electroporation conditions for the transformation of mammalian cells. *Methods Mol Biol* **130:** 117–134.

Janke, C., Magiera, M.M., Rathfelder, N., Taxis, C., Reber, S., Maekawa, H., *et al*. (2004) A versatile toolbox for PCR-based tagging of yeast genes: new fluorescent proteins, more markers and promoter substitution cassettes. *Yeast* **21:** 947–962.

Klauer, A.A., and van Hoof, A. (2012) Degradation of mRNAs that lack a stop codon: a decade of nonstop progress. *Wiley Interdiscip Rev RNA* **3:** 649–660.

Kiethega, G.N., Yan, Y., Turcotte, M., and Burger, G. (2013) RNA-level unscrambling of fragmented genes in *Diplonema* mitochondria. *RNA Biol* **10:** 301–313.

Lai, D.H., Hashimi, H., Lun, Z.R., Ayala, F.J., and Lukeš, J. (2008) Adaptations of *Trypanosoma brucei* to gradual loss of kinetoplast DNA: *Trypanosoma equiperdum* and *Trypanosoma evansi* are *petite* mutants of *T. brucei*. *Proc Natl Acad Sci U S A* **105:** 1999–2004.

Lai, J., Ng, S.K., Liu, F.F., Patkar, R.N., Lu, Y., Chan, J.R., *et al*. (2010) Marker fusion tagging, a new method for production of chromosomally encoded fusion proteins. *Eukaryot Cell* **9:** 827–830.

Lander, N., Chiurillo, M.A., and Docampo, R. (2016) Genome editing by CRISPR/Cas9: A game change in the genetic manipulation of protists. *J Eukaryot Microbiol* **63:** 679–690.

Lara, E., Moreira, D., Vereshchaka, A., and López-García, P. (2009) Panoceanic distribution of new highly diverse clades of deep-sea diplonemids. *Environ Microbiol* **11:** 47–55.

Larsen, J., and Patterson, D.J. (1990) Some flagellates (Protista) from tropical marine sediments. *J. Nat. Hist* **24:** 801–937.

Lukeš, J., Flegontova, O., and Horák, A. (2015) Diplonemids. *Curr Biol* **25:** R702–R704.

Makiuchi, T., Annoura, T., Hashimoto, M., Hashimoto, T., Aoki, T., and Nara, T. (2011) Compartmentalization of a glycolytic enzyme in *Diplonema*, a non-kinetoplastid euglenozoan. *Protist* **162:** 482–489.

Marande, W., and Burger, G. (2007) Mitochondrial DNA as a genomic jigsaw puzzle. *Science* **318:** 415.

Marande, W., Lukeš, J., and Burger, G. (2005) Unique mitochondrial genome structure in diplonemids, the sister group of kinetoplastids. *Eukaryot Cell* **4:** 1137–1146.

Michael, R. (2010) The mechanism of double-strand DNA break repair by the nonhomologous DNA end joining pathway. *Annu Rev Biochem* **79:** 181–211.

Morales, J., Hashimoto, M., Williams, T.A., Hirawake-Mogi, H., Makiuchi, T., Tsubouchi, A., *et al*. (2016) Differential remodelling of peroxisome function underpins the environmental and metabolic adaptability of diplonemids and kinetoplastids. *Proc Biol Sci* **283:** 20160520.

Moreira, S., Valach, M., Aoulad-Aissa, M., Otto, C., and Burger, G. (2016) Novel modes of RNA editing in mitochondria. *Nucleic Acids Res* **44:** 4907–4919.

Pestka, S. (1971) Inhibitors of ribosome functions. *Annu Rev Microbiol* **25:** 487–562.

Porter, D. (1973) *Isonema papillatum* sp. n., a new colorless marine flagellate: a light- and electron microscopic study. *J Protozool* **20:** 351–356.

Potter, H., and Heller, R. (2003) Transfection by electroporation. *Curr Protoc Mol Biol* Chapter 9, Unit-9.3.

Räz, B., Iten, M., Grether-Bühler, Y., Kaminsky, R., and Brun, R. (1997) The Alamar Blue assay to determine drug sensitivity of African trypanosomes (*T.b. rhodesiense* and *T.b. gambiense*) in vitro. *Acta Trop* **68:** 139–147.

Roy, J., Faktorová, D., Benada, O., Lukeš, J., and Burger, G. (2007) Description of *Rhynchopus euleeides* n. sp. (Diplonemea), a free-living marine euglenozoan. *J Eukaryot Microbiol* **54:** 137–145.

Sargent, R.G., Brenneman, M.A., and Wilson, J.H. (1997) Repair of site-specific double-strand breaks in a mammalian chromosome by homologous and illegitimate recombination. *Mol Cell Biol* **17:** 267–277.

Schnepf, E. (1994) Light and electron microscopical observations in *Rhynchopus coscinodiscivorus* spec. nov., a colorless, phagotrophic Euglenozoon with concealed flagella. *Arch Protistenkd* **144:** 63–74.

Schuster, F.L., Goldstein, S., and Hershenov, B. (1968) Ultrastructure of a flagellate, *Isonema nigricans* nov. gen. nov. sp., from a polluted marine habitat. *Protistologica* **4:** 141–149.

Sheriff, O., Lim, L.F., and He, C.Y. (2014) Tracking the biogenesis and inheritance of subpellicular microtubule in *Trypanosoma brucei* with inducible YFP-α-tubulin. *Biomed Res Int* **2014:** 893272.

Simpson, A.G.B. (1997) The identity and composition of the Euglenozoa. *Arch Protistenkd* **148:** 318–328.
Skuja, H. (1948) Taxonomie des phytoplanktons einiger seen in Uppland, Schweden. *Symb Bot Upsal* **9:** 5–399.
Stretton, S., Techkarnjanaruk, S., McLennan, A.M., and Goodman, A.E. (1998) Use of green fluorescent protein to tag and investigate gene expression in marine bacteria. *Appl Environ Microbiol* **64:** 2554–2559.
Sturm, N.R., Maslov, D.A., Grisard, E.C., and Campbell, D.A. (2001) *Diplonema* spp. possess spliced leader RNA genes similar to the Kinetoplastida. *J Eukaryot Microbiol* **48:** 325–331.
Tashyreva, D., Prokopchuk, G., Yabuki, A., Kaur, B., Faktorová, D., Votýpka, J., *et al.* (2018) Phylogeny and morphology of diplonemids from the Sea of Japan. *Protist* (in press).
Valach, M., Moreira, S., Faktorová, D., Lukeš, J., and Burger, G. (2016) Post-transcriptional mending of gene sequences: Looking under the hood of mitochondrial gene expression in diplonemids. *RNA Biol* **13:** 1204–1211.
van den Hoff, M.J.B., Moorman, A.F.M., and Lamers, W.H. (1992) Electroporation in 'intracellular' buffer increases cell survival. *Nucleic Acids Res* **20:** 2902.
van Ooijen, G., Knox, K., Kis, K., Bouget, F.Y., and Millar, A.J. (2012) Genomic transformation of the picoeukaryote *Ostreococcus tauri*. *J Vis Exp* **65:** 4074.
Vondrušková, E., Van Den Burg, J., Zíková, A., Ernst, N., Stuart, K., Benne, R., and Lukeš, J. (2005) RNA interference analyses suggest a transcript-specific regulatory role for mitochondrial RNA-binding proteins MRP1 and MRP2 in RNA editing and other RNA processing in *Trypanosoma brucei*. *J Biol Chem* **280:** 2429–2438.
Wang, Q., Xue, H., Li, S., Chen, Y., Tian, X., Xu, X., *et al.* (2017) A method for labeling proteins with tags at the native genomic loci in budding yeast. *PLoS One* **12:** e0176184.
Worden, A.Z., and Wilken, S. (2016) A plankton bloom shifts as the ocean warms. *Science* **354:** 287–288.
Yabuki, A., and Tame, A. (2015) Phylogeny and reclassification of *Hemistasia phaeocysticola* (Scherffel) Elbrachter & Schnepf, 1996. *J Eukaryot Microbiol* **62:** 426–429.
Yabuki, A., Tanifuji, G., Kusaka, C., Takishita, K., and Fujikura, K. (2016) Hyper-eccentric structural genes in the mitochondrial genome of the algal parasite *Hemistasia phaeocysticola*. *Genome Biol Evol* **8:** 2870–2878.

## Supporting information

Additional Supporting Information may be found in the online version of this article at the publisher's web-site:

**Table S1**. List of primers used.

**Fig. S1.** PCR amplicons (from Fig. 3B) obtained with primers that amplify the puromycin$^R$ region (A) or mCherry region (B) of clones A3 and A4 were verified by sequencing. Beginning parts of the amplicon sequences are aligned with the reference sequence.

**Fig. S2.** SL-PCR amplicons (from Fig. 4C) were verified by sequencing. Part of the amplicon sequences obtained with primers that amplify the puromycin$^R$ region (A) or mCherry region (B) are aligned to the reference sequence.

**Fig. S3.** Western blot analysis of wild type (WT) *D. papillatum* and transformants A3 and A4 after 24 h incubation in a medium containing 20 μg/ml puromycin. *Trypanosoma brucei* SMOX P9 procyclic stage cells (SmOx) expressing the puromycin$^R$ gene were used as a positive control. Monoclonal mouse anti-Puromycin antibodies (1:1000) and secondary anti-mouse antibodies coupled to horseradish peroxidase (1:1000) were used for visualization employing the ECL kit.

**Fig. S4.** Confirmation that the electroporated construct is integrated in the *D. papillatum* genome. (A) Scheme of the puromycin$^R$ (puro$^R$) + mCherry cassette (2995 bp *Not*I fragment) including restriction sites, positions of the primers and expected sizes of the amplicons. The whole gels with PCR of total DNA of *D. papillatum* wild type (WT), selected transformants (A3 and A4; underlined) and some other obtained transformants (A2, A5, B4, D2, B2, C2) using specific primers for amplification of puromycin$^R$ (B), mCherry (C) or puromycin$^R$ + mCherry (D). Negative control PCR (NC) was performed without template DNA.

**Fig. S5.** Validation of proper transcription and post-transcriptional 5′ end-processing of the transcripts produced from heterologous genes in *D. papillatum*. (A) The whole gels of RT-PCR shown in Fig. 4B. RNA from *D. papillatum* wild type (WT) and selected transformants (A3 and A4; underlined) and some other obtained transformants (C3, B3, B4, A5) was used as a template for RT-PCR. Expected sizes of the RT-PCR products are indicated. Reactions with reverse transcriptase added and negative controls without reverse transcriptase are indicated by (+) and (-). (B) The amplification of the 5′ region from the puromycin$^R$ (puro$^R$) transcript and the mCherry transcript respectively. Nested SL RT-PCR using total RNA from the transformants A3 and A4 as templates, and two sets of primers that anneal to the conserved SL sequence of *D. papillatum* (forward primers) and to the 5′ end of the transcripts (reverse primers), see Fig. 4A. The whole gels of both SL RT-PCR reaction are shown here together with the sizes of expected product.

**Fig. S6.** Whole gels of western blot analysis (shown in Fig. 5) of *D. papillatum* wild type (WT) and transformants A3 and A4 that express the puromycin$^R$ gene (puromycin N-acetyltransferase). Monoclonal rabbit anti-Puromycin N-acetyltransferase antibodies (1:500) and secondary anti-rabbit antibodies coupled to horseradish peroxidase (1:1,000). 29-13, *T. brucei* procyclic-stage cell line 29-13, which does not express the puromycin$^R$ gene, is used as a negative control. SMOX, *T. brucei* cell line SMOX P9, which does express the puromycin$^R$ gene, is used as a positive control. Anti-α-tubulin antibodies were used as a loading control.